

Long ligands reinforce biological adhesion under shear flow

Aleksey V. Belyaev*

M.V. Lomonosov Moscow State University, Faculty of Physics, 119991 Moscow, Russia

(Dated: December 3, 2024)

In the present work the computer modelling was used to show that longer ligands allow biological cells (e.g. blood platelets) to withstand stronger flows after their adhesion to solid walls. Mechanistic model of polymer-mediated ligand-receptor adhesion between a microparticle (cell) and a flat wall was developed. Theoretical threshold between adherent and non-adherent regimes was derived analytically and approved by the simulations. These results lead to deeper understanding of numerous biophysical processes, e.g. arterial thrombosis, and to the design of new biomimetic colloid-polymer systems.

PACS numbers: 87.17.Rt, 87.17.Aa, 87.15.Fh

Adhesion is ubiquitous in different fields of physics, material science, physical chemistry, and biology. The mechanisms of sticking may be complex and involve various physical interactions, roughness and friction, etc. [1–3] Unlike non-living matter, the biological cells often rely on “key-lock” ligand-receptor binding involving special membrane-anchored proteins - cell adhesion molecules (CAMs) - and the adhesive substrate, e.g. extracellular matrix, collagen, or other another cell [4–7]. The importance of adhesion in biological systems is supported by numerous examples, such as the formation and growth of bacterial clusters and biofilms [8] on medical implants [9], sticking of blood cells to endothelial lining of blood vessels during haemostatic [10] and immune response [11, 12], tissue formation, etc. The adhesion should be reliable and adjustable, especially when the cells are supposed to function in strong hydrodynamic flows [13–16]. One of the most intriguing examples is the adhesion of blood platelets to the damaged blood vessel during haemostatic process. It is provided by the reversible binding between GPIb-IX-V receptor complex on the platelet membrane and protein ligand von Willebrand factor (vWf). Normally vWf exists in a form of long chains called “multimers”, which provide platelet aggregation in case of severe bleeding [17]. In some cases these aggregates can obstruct blood vessels, dangerously limiting the blood circulation and causing the thrombosis. Understanding of mechanics and regulation of this phenomenon may help to develop the anti-thrombotic therapy and laboratory tests [18], hemocompatible materials for implants [19] and design biomimetic colloidal-polymer systems [20].

Prior models [12, 21–26] and experiments [27–29] underlined the role of reaction rates and loading forces on the dynamics of blood cells subjected to microvascular and arterial flow conditions. Number of models of leukocyte rolling assumed that the ligand length was small compared to cell diameter [30, 31]. Apparently this is not the case for vWf-mediated adhesion and aggregation of platelets. One of the essential features of vWf

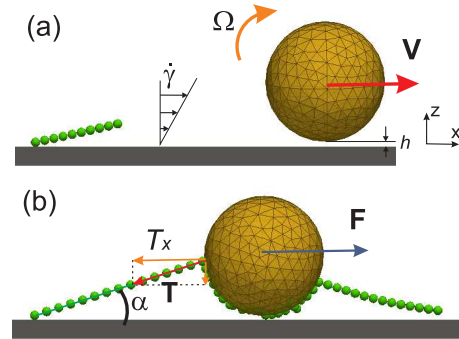


FIG. 1. Illustration of the polymer-mediated adhesion mechanics. (a) In the shear flow a spherical particle is rolling and translating along the wall within a distance h . The tether can stick to the sphere (b), and if the tether is long enough, it develops a sufficient tension force $T \cos \alpha$ to hold the sphere against the drag force F . Yet if α is too big, then the maximal tension T_{\max} is reached and the tether detaches (a).

is that these proteins can expand due to the blood flow up to several micrometers in length [32–35] and capture the platelets separated by long distances. This protein is also responsible for preventing bleeding by sticking blood platelets to the extracellular matrix or damaged blood vessel walls [28, 36, 37]. It is known that the deficiency of vWf concentration in blood causes bleeding disorder, as well as the short length of these macromolecular ligands [38]. At the same time, ultra-long vWf chains may cause thrombotic conditions [39]. The role of the ligand length in cell adhesion to walls needs to be studied and quantified. The questions are why long tethers are required for efficient blood cell adhesion in flow and how long should these tethers be to accomplish their physiological role. In the present work these issues have been addressed by the means of the computer simulations.

The adhesion of a microscopic colloid (cell) to a flat wall via binding to a polymer ligand in Couette flow was studied. A basic mechanical model was used for theoretical description. Consider a spherical particle retained against hydrodynamic forces by the polymer near a solid impenetrable wall (Fig.1). Let us denote the cell radius

* aleksey_belyaev@yahoo.com

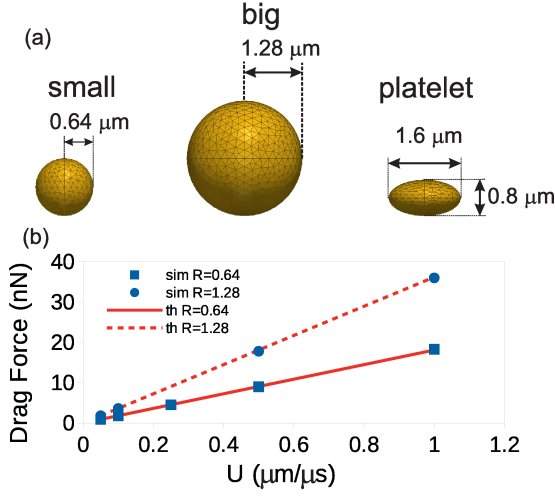


FIG. 2. (a) Three types of particles used in the present work. (b) Drag on a sphere held against the flow with constant velocity U . Numerical results (squares - for the smaller sphere, circles - for the bigger one) agree with Stokes's law (lines).

as R and the tether length as L . In case of a long ligand ($R/L \ll 1$) the cell could be represented as a material point. The force balance requires that $F = T \cos \alpha$, where T is the tension force of the tether and $F = A \cdot R^2 \dot{\gamma}$ is the hydrodynamic drag force with $\dot{\gamma}$ being the near-wall shear rate. The coefficient A depends on the dynamic viscosity μ of the fluid, the shape of the particle and the nearness of the walls. According to the Goldmann-Cox-Brenner theory [40], $A \approx 1.7 \cdot 6\pi\mu$. The tethering polymer can detach from the sphere if T exceeds some threshold value T_{\max} . The tethering angle α could be determined from the condition that the non-deformed sphere touches the wall, so that $\sin \alpha \approx R/L$. This results in the following expression for the critical shear rate

$$\dot{\gamma}_{\text{cr}} = \frac{T_{\max}}{AR^2} [1 - (R/L)^2], \quad (1)$$

so that the adhesion is firm if $\dot{\gamma} \leq \dot{\gamma}_{\text{cr}}$ and impossible otherwise. In the opposite case of a short ligand ($R/L \gg 1$) the size of the cell becomes substantial, so the corrected formula reads [41]

$$\dot{\gamma}_{\text{cr}} = \frac{T_{\max}}{AR^2} \left[1 - \left(\frac{R}{L+R} \right)^2 \right]. \quad (2)$$

From these expressions we see the advantages of longer ligands: they increase the projection $T_x = T \cos \alpha$ of the tension force \mathbf{T} that counterbalances the hydrodynamic drag force \mathbf{F} (Fig.1). This hypothesis has been verified by computer simulations in the present work.

3D computer model was developed on the basis of the open-source package ESPResSo (version 3.4). A hybrid Lattice Boltzmann (LB) - Lagrangian Particle Dynamics (LPD) model has been employed [43, 44]. The dimensionless values were used for convenience so that $[L] = 1 \mu\text{m}$,

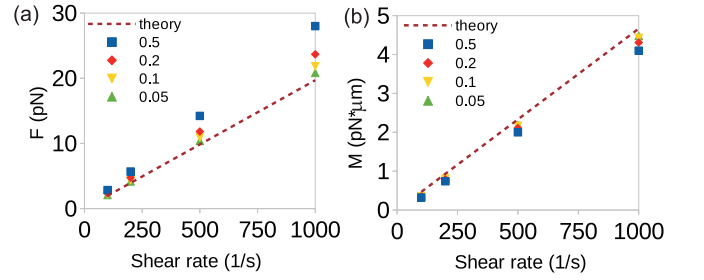


FIG. 3. Drag force (left panel) and torque (right) on the immobile sphere ($R = 0.64 \mu\text{m}$) near wall in shear flow. Symbols correspond to simulation results for different distances h between the sphere and the wall, lines - to the analytical formulas from [40, 42].

$[F] = 1 \text{ nN}$, $[t] = 1 \mu\text{s}$. Lattice Boltzmann BGK-scheme was used to simulate low-Reynolds number hydrodynamics of a viscous fluid in the simulation box [45]. Each adherent object (sphere or platelet) immersed into the fluid was represented by a mesh of Lagrangian surface points connected by elastic bonds [44]. Molecular dynamics (MD) approach was used to track cell motion in time. The coupling between fluid flow and cell membrane was introduced by a viscous drag force $\mathbf{F}_j = -\xi \Delta \mathbf{u}_j$ exerted on the cell membrane nodes. The hydrodynamic part of the model has been successfully used in prior works [44, 46]. The ligand polymer (tether) was attached to the bottom surface by one of its ends and stretched along the x-axis. After that a short equilibration run (500 μs) was performed before each simulation. The polymer was modelled as a chain of N beads of radius $a = 0.05$ connected with springs. Non-linear FENE potential was used for springs [47].

Spheres of two sizes were used: $R = 0.64 \mu\text{m}$ and $1.28 \mu\text{m}$. The platelet was equivolume to the smaller sphere and had a realistic 2:1 aspect ratio, Fig.2(a). In order to ensure that the model gives correct values of drag forces and torques, validation tests were performed. A non-deformable sphere was placed into a simulation box in different flow setups. The total drag force F and torque M on the sphere were measured in simulations. The first test was based on a well-known Stokes drag formula: $F_{\text{Stokes}} = 6\pi\mu RU$. The sphere was placed into the center of the simulation box and immobilized, and a constant velocity condition $(U, 0, 0)$ was imposed on the boundaries of the box. The results of this test in Fig.2(b) show a reasonable agreement with Stokes's law. Additionally, a set of validation runs was performed for the sphere near a flat wall in a shear flow, Fig.3, and compared to known theoretical expressions [40, 42]. According to these results, the hydrodynamic accuracy of the model is quite good.

The first set of results corresponds to the spheres. In the beginning of each simulation the sphere was placed within a distance $h_0 = 2a$ from the wall. A big set of simulations allowed to plot a map of adhesion regimes

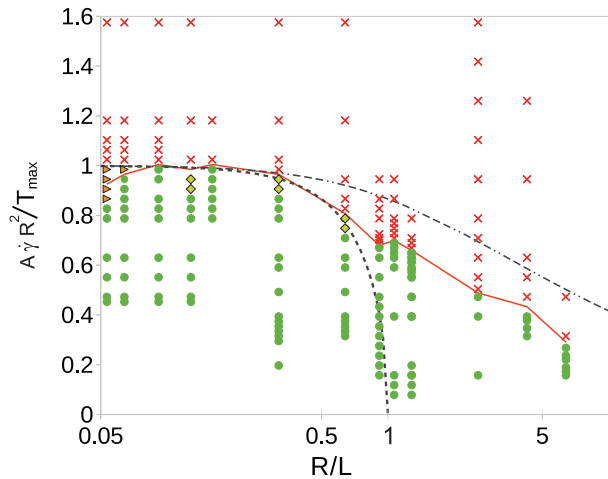


FIG. 4. Adhesion regimes diagram: red crosses correspond to cases when the tether was unable to hold the sphere; green circles - when sphere remained attached by the end of simulation; orange triangles - to rolling with stops; light green diamonds - to adhesion when the tethering occurred on the second (or third, etc.) approach. Dashed line corresponds to Eq.(1) and dash-dotted line - to Eq.(2). Solid red line is the eye-guide for the boundary between adhesive and non-adhesive regimes.

(Fig. 4). Here, as the theory suggests, the increase of the cell size R relatively to the contour length of the tether-polymer ($L = N \cdot r_0$) causes the breakage of the adhesive bond at lower shear rates. The simulations support this idea, as seen in Fig. 4 (see also *Supplementary Movies 1* and 2). When the ratio is small $R/L \ll 1$, the threshold of stable adhesion is the highest, as predicted by Eq.(1), and it only slightly depends on R/L . For a sphere with $R = 0.64 \mu\text{m}$ the threshold shear rate between the firmly adherent state and the free-flowing regime is approximately 1200 s^{-1} . If $R/L \gg 1$, the maximal force that a bond can sustain falls rapidly to zero (in simulations it decreases even faster than predicted by Eq.(2)). For ultra-long chains ($N \geq 100$, $R/L < 0.06$) there was observed an intermediate regime: slow rolling with halts and re-initiation of motion. Apparently, when the force balance is reached, the cell stops. But due to rotation of the sphere around x-axis, the equilibrium crashes, and the cell rolling starts again (see *Supplementary Movie 3*).

Mean velocity of the cell was measured during the timespan 100 ms after the start for each simulation. Simulation snapshots, Fig.5(a), show the initial stages of adhesion. In the beginning the tension force T_x component (parallel to the wall) is minimal. As the cell moves along the flow, the tethering angle α sharpens. Ideally, $\alpha \rightarrow 0$ for $R/L \rightarrow 0$. Yet if T_{max} is not sufficient to hold the cell attached to the wall for a given $L = Nr_0$, the tether breaks and the cell starts flowing with the fluid. It was found that longer ligands indeed help to withstand more intensive flows, Fig.5(b). Negligible mean velocity corresponds to lasting adhesion. The transition between

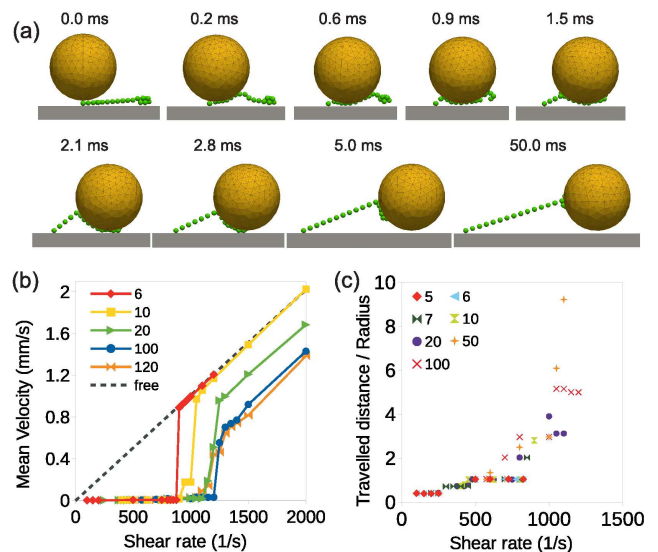


FIG. 5. (a) Series of simulation shots for $R = 0.64 \mu\text{m}$, $N = 20$, $\dot{\gamma} = 10^3 /\text{s}$. (b) Mean velocity of the sphere ($R = 0.64$) plotted versus shear rate for different N . Dashed line corresponds to the theoretical velocity $V = \dot{\gamma}(R + h)$ of a free-flowing sphere at distance $h = 0.15 \mu\text{m}$ from the wall. (c) Distance travelled by the sphere ($R = 0.64 \mu\text{m}$) before stoppage in cases of durable adhesion for different N .

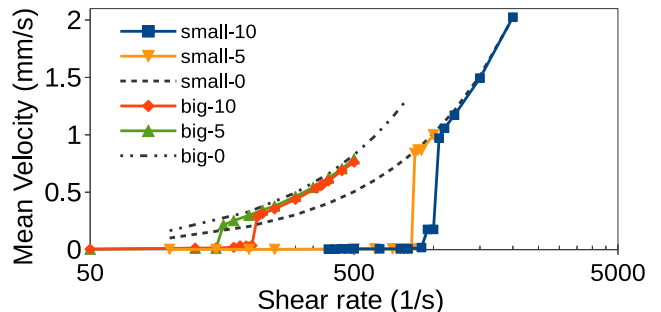


FIG. 6. Mean velocity of a sphere versus shear rate depending on N and R . Lines correspond to theoretical velocity of a free-flowing sphere.

adhesion regimes shifts to greater shear rates for longer polymers, in accordance with the theoretical prediction. Longer linkers (> 10 monomers) also decelerate the cell even in the no-adhesion regime, for there exists a period of a slow rolling of a sphere over the polymer chain before the detachment. The longer the chain, the longer this period. The distance travelled by the cell until the stoppage increases non-linearly with the shear rate in cases of stable adhesion, Fig.5(c).

The value of the bond-rupturing shear rate $\dot{\gamma}_{\text{cr}}$ depends strongly on the cell size: if we double the sphere radius, then the drag will increase 4 times (as $F_{\text{drag}} \propto \dot{\gamma}R^2$). Therefore, for the same detachment force T_{max} and the same R/L (i.e. double the length of ligand together with the radius) the critical shear rate for the big cell should

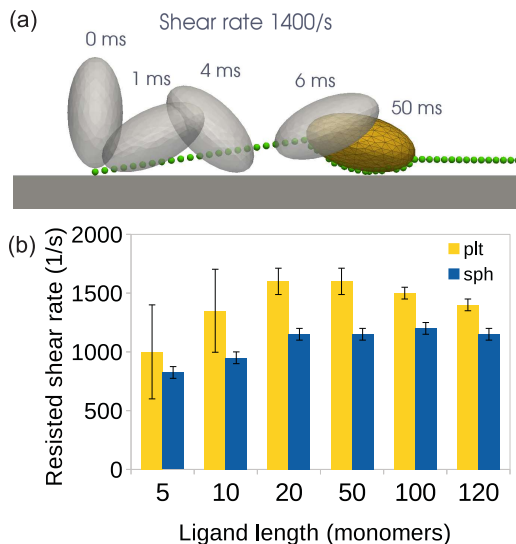


FIG. 7. (a) Simulation of the platelet motion before adhering to wall via binding with grafted von Willebrand factor chain. (b) Diagram comparing the maximal shear rate sustained by the platelet (yellow) and the equivolume sphere (blue). For platelet the error bars correspond to deviation due to its initial placement (different orientation of symmetry axis), and for the sphere - to half of the step for the shear rate (50 s^{-1}) between two consequent simulations.

be 4 times smaller as compared to the small one. This was observed in the simulations (Fig.6): for the small sphere and 5-monomers long ligand $\dot{\gamma}_{cr} \approx 850 \text{ s}^{-1}$, while for the big sphere and 10-monomers long ligand $\dot{\gamma}_{cr} \approx 215 \text{ s}^{-1}$. Noteworthy, if the ligand length is kept the same, then $\dot{\gamma}_{cr}$ decreases even more: for $R = 1.28 \text{ }\mu\text{m}$ and $N = 5$ the maximal shear rate is 160 s^{-1} . This means

that longer polymers are required to hold bigger cells against the stream (see *Supplementary Movie 4*). The blood platelets have typical sizes of 1-2 microns and the adhesive ligand (von Willebrand factor) could be 20-50 monomers long (on average), which, as the simulations suggest, is quite enough to withstand drag at wall shear rate of $1000\text{-}1200 \text{ s}^{-1}$.

Blood platelets are not spherical: normally they are oblate spheroids, thus their name. In order to investigate the effect of cell shape, the simulations with a platelet-shaped particle were also performed in a range of shear rates. Different ligand lengths and different initial placements of the platelet were used. In particular, the platelets demonstrate a more complicated motion as compared to spheres [48]. Due to the shape and the non-penetration condition the center of mass of the platelet jumps and falls during the rolling over the adhesive wall Fig.7(a), in contrast to sphere. The results of the simulations, presented in Fig.7(b), suggest that platelets can sustain greater wall shear rates as compared to spheres. The reason is their streamlined shape, lower profile and, consequently, smaller drag force (see *Supplementary Movie 5*).

In conclusion, the present study shows that longer tethers are preferable for adhesion of blood platelets to injury, thrombus or extracellular matrix due to more favourable direction of tether tension force. The oblate shape and small size allow platelets to minimize the drag and promote aggregation. Hopefully, these findings would deepen the physical insight into physiological phenomena that rely on cell adhesion, e.g. thrombosis and hemostasis.

This research was supported by Russian Science Foundation (project number 17-71-10150). The simulations were carried out using computational resources of the Supercomputing Center of M. V. Lomonosov Moscow State University (“Lomonosov” and “Lomonosov-2”) [49].

-
- [1] M. Mani, A. Gopinath, and L. Mahadevan, *Phys. Rev. Lett.* **108**, 226104 (2012).
 - [2] Y.-S. Chu, S. Dufour, J. P. Thiery, E. Perez, and F. Pincet, *Phys. Rev. Lett.* **94**, 028102 (2005).
 - [3] K. L. Johnson, K. Kendall, and A. D. Roberts, *Proc. R. Soc. Lond. A* **324**, 301 (1971).
 - [4] T. R. Weigl, M. Asfaw, H. Krobath, B. Rozycki, and R. Lipowsky, *Soft Matter* **5**, 3213 (2009).
 - [5] S. Rakshit and S. Sivasankar, *Phys. Chem. Chem. Phys.* **16**, 2211 (2014).
 - [6] W. Thomas, E. Trintchina, M. Forero, V. Vogel, and E. Sokurenko, *Cell* **109**, 913 (2002).
 - [7] D. Hammer and D. Lauffenburger, *Biophysics Journal* **52**, 475 (1987).
 - [8] S. Sircar and D. M. Bortz, *Mathematical Biosciences* **245**, 314 (2013).
 - [9] K. K. Chung, J. F. Schumacher, E. M. Sampson, R. A. Burne, P. J. Antonelli, and A. B. Brennan, *Biointerfaces* **2**, 89 (2007).
 - [10] M. J. E. Kuijpers, K. Gilio, S. Reitsma, R. Nergiz-Unal, L. Prinzen, S. Heeneman, E. Lutgens, M. van Zanvoort, B. Neiswandt, M. O. Egbrink, and J. Heemskerk, *J. Thromb. Haemost.* **7**, 152 (2009).
 - [11] M. B. Lawrence and T. A. Springer, *Cell* **65**, 859 (1991).
 - [12] V. P. Kristina D. Rinker and G. A. Truskey, *Biophysical Journal* **80**, 1722 (2001).
 - [13] N. Begent and G. V. R. Born, *Nature* **227**, 926 (1970).
 - [14] A. V. Belyaev, M. A. Panteleev, and F. I. Ataullakhanov, *Biophysical Journal* **109**, 450 (2015).
 - [15] I. V. Pivkin, P. D. Richardson, and G. Karniadakis, *Proc. Nat. Acad. Sci.* **103**, 17164 (2006).
 - [16] Z. Xu, N. Chen, S. C. Shadden, J. E. Marsden, M. M. Kamocka, E. D. Rosen, and M. Alber, *Soft Matter* **5**, 769 (2009).
 - [17] T. A. Springer, *Cell* **124**, 1412 (2014).
 - [18] T. Colace, J. Jobson, and S. Diamond, *Bioconjug Chem* **22**, 2104 (2011).
 - [19] P. Goodman, E. Barlow, P.M.Crapo, S.F.Mohammad,

- and K. Solen, *Annals of Biomedical Engineering* **33**, 780 (2005).
- [20] H. Chen, M. A. Fallah, V. Huck, J. I. Angerer, A. J. Reininger, S. W. Schneider, M. F. Schneider, and A. Alexander-Katz, *Nature Communications* **4**, 1333 (2013).
- [21] C. Pozrikidis, *J Fluid Mech.* **568**, 161 (2005).
- [22] W. Wang, N. A. Mody, and M. R. King, *J Comput Phys.* **244**, 223 (2013).
- [23] N. A. Mody and M. R. King, *Biophys. J.* **95**, 2556 (2008).
- [24] Z. Y. Luo and B. F. Bai, *Soft Matter* **12**, 6918 (2016).
- [25] G. B. Chapman and G. R. Cokelet, *Biophysical Journal* **74**, 3292 (1998).
- [26] E. F. Krasik and D. A. Hammer, *Biophysical Journal* **87**, 2919 (2004).
- [27] J. Kim, C.-Z. Zhang, X. Zhang, and T. A. Springer, *Nature* **466**, 992 (2010).
- [28] L. A. Coburn, V. S. Damaraju, S. Dozic, S. G. Eskin, M. A. Cruz, and L. V. McIntire, *Biophysical Journal* **100**, 304 (2011).
- [29] J. Piper, R. Swerlick, and C. Zhu, *Biophysics Journal* **74**, 492 (1998).
- [30] D. Hammer and S. Apte, *Biophysics Journal* **63**, 35 (1992).
- [31] S. Reboux, G. Richardson, and O. Jensen, *Proc. R. Soc. A* **464**, 447 (2008).
- [32] H. Slayter, J. Loscalzo, P. Bockenstedt, and R. I. Handin, *Journal of Biological Chemistry* **260**, 8559 (1985).
- [33] L. Novák, H. Deckmyn, S. Damjanovich, and J. Hársfalvi, *Blood* **99**, 2070 (2002).
- [34] S. Schneider, S. Nuschele, A. Wixforth, C. Gorzelanny, A. Alexander-Katz, R. R. Netz, and M. F. Schneider, *PNAS* **104**, 7899 (2007).
- [35] K. Rack, V. Huck, M. Hoore, D. Fedosov, S. Schneider, and G. Gompper, *Scientific Reports*, **7**, 14278 (2017).
- [36] S. P. Jackson, W. S. Nesbitt, and E. Westein, *Journal of Thrombosis and Haemostasis* **7**, 17 (2009).
- [37] T. Yago, J. Lou, T. Wu, J. Yang, J. J. Miner, L. Coburn, J. A. Lopez, M. A. Cruz, J.-F. Dong, L. V. McIntire, R. P. McEver, and C. Zhu, *J. Clin. Invest.* **118**, 3195 (2008).
- [38] C. Denis, N. Methia, P. S. Frenette, H. Rayburn, M. Ullman-Culleré, R. O. Hynes, and D. D. Wagner, *Proc. Natl. Acad. Sci. USA* **95**, 9524 (1998).
- [39] J.-f. Dong, J. L. Moake, L. Nolasco, A. Bernardo, W. Arceneaux, C. N. Shrimpton, A. J. Schade, L. V. McIntire, K. Fujikawa, and J. A. López, **100**, 4033 (2002).
- [40] A. J. Goldman, R. G. Cox, and H. Brenner, *Chem. Eng. Sci.* **22**, 653 (1967).
- [41] Strictly speaking, the rotation of the cell should be taken into account from the balance of torques. But for spherical cells it only lifts the point of polymer-to-cell attachment to a distance $\approx R$ from the wall, as observed in the simulations.
- [42] M. E. O'Neill, *Chem. Eng. Sci.* **23**, 1293 (1968).
- [43] B. Dunweg and A. J. C. Ladd, in *Adv. in Polymer Sci.* (Springer Berlin Heidelberg, 2008) pp. 1–78.
- [44] I. Cimrak, M. Gusenbauer, and T. Schrefl, *Computers and Mathematics with Applications* **64**, 278 (2012), mathematical Methods and Models in Biosciences.
- [45] S. Succi, *The Lattice Boltzmann Equation for Fluid Dynamics and Beyond (Numerical Mathematics and Scientific Computation)* (Oxford University Press, USA, 2001).
- [46] A. V. Belyaev, *PLoS ONE* **12**, e0183093 (2017).
- [47] See Supplemental Material at [URL will be inserted by publisher] for the details of the computer model and the captions for the Supplemental Movies.
- [48] C. Pozrikidis, *J. Fluid Mech.* **541**, 105 (2005).
- [49] V. V. Voevodin, S. A. Zhumatiy, S. I. Sobolev, A. S. Antonov, P. A. Bryzgalov, D. A. Nikitenko, K. S. Stefanov, and V. V. Voevodin, *Open Systems J.*, 36 (2012), in Russian.